Optimized all-optical amplitude reshaping by exploiting nonlinear phase shift in fiber for degenerated FWM

Heng Zhou (周 恒)*, Kun Qiu (邱 昆), and Fengfeng Tian (田丰沣)

Key Lab of Optical Fiber Sensing and Communication Networks, Ministry of Education, University of Electronic Science and Technology of China, Chengdu 611731, China

**Corresponding author: zhouheng830813@163.com*

Received September 20, 2011; accepted November 30, 2011; posted online January 17, 2012

We describe a novel performance optimization method for all-optical amplitude reshaping via degenerated four-wave mixing (FWM) in highly nonlinear optical fiber. The proposed optimization method is achieved by judiciously configuring the FWM operational condition and exploiting the nonlinear phase shift induced by self- and cross-phase modulations to properly influence the FWM conversion efficiency. Through the proposed scheme, fully functional and prevailing reshaping performance, including significant amplitude jitter suppression and extinction ratio improvement, is obtained within a single FWM stage. Results of the present theoretical calculation and numerical simulation verify the feasibility and advantages of the proposed scheme.

OCIS codes: 060.1115, 060.2310, 060.4370, 060.7140.

doi: 10.3788/COL201210.050601.

All-optical 3R regeneration, which implements signal reamplification, reshaping, and retiming to mitigate the accumulated transmission impairments in the optical domain and avoid the demanding O/E/O conversion, is now considered as one of the elemental functions for future high speed all-optical networks[1]. As a fundamental aspect of 3R regeneration, all-optical amplitude reshaping has been subject to extensive theoretical and experimental studies during the last decade[1−7]. Generally, all-optical amplitude reshaping for ultrahigh speed optical signal (>40 Gb/s) is achieved using various quasi-instantaneous nonlinear optical effects to construct an S-shaped power transfer function (PTF) between the input and output signals in order to fulfill signal extinction ratio (ER) improvement and amplitude jitter (AJ) suppression. Previously reported schemes include self-phase modulation (SPM) based on spectral broadening and off-center filtering[1], cross-phase modulation (XPM) in a nonlinear optical loop mirror[2], and optical parametric amplifying and four-wave mixing (FWM)[3−7]. Among these schemes, the FWM-based scheme is considered an attractive candidate owing to its transparency to data bitrates and duty cycles and capability of simultaneous amplitude reshaping, signal retiming, and wavelength conversion[3]. In Refs. [4,5], all-optical amplitude reshaping based on FWM has been initially proposed and demonstrated using higher-order FWM idler wave generation in dispersion shift fiber. In the scheme, signal ER improvement is realized by the nonlinear amplitude stretching of the higher-order FWM idler wave, and the AJ suppression on marks is achieved via the pump depletion effect. The main drawback of this scheme is that higher-order FWM idler wave generation suffers from low efficiency and consequently requires very large pumping power. In Ref. [6], a pump-modulated scheme is proposed to achieve all-optical amplitude reshaping using a lower-order FWM idler wave with lower pump power requirement. However, this scheme obtains limited reshaping performance due to the insufficient nonlinear amplitude stretching of the lower-order FWM idler wave. Favorable all-optical amplitude reshaping has been reported using cascaded FWM stages[6,7] but at the expense of increased system component count and cost.

In this letter, a performance optimization method for FWM-based all-optical amplitude reshaping is described and verified. The proposed scheme exploits SPM- and XPM-induced nonlinear phase shifts to properly control the FWM conversion efficiency and to construct an enhanced S-shaped PTF for eventual amplitude reshaping.

The configuration of the proposed scheme is identical with former FWM-based all-optical amplitude reshaper, as shown in the upper diagram of Fig. 1. An amplitude modulated data wave U_1 and a continuous wave U_2 are sent into a highly nonlinear fiber (HNLF), where degenerated FWM occurs and new idler waves are generated. Here the modulated wave U_1 acts as the pump wave, and the continuous wave U_2 acts as the signal wave in the FWM process[6]; idler wave U_3 is filtered out as the reshaped data by an optical band pass filter (BPF) assigned after the HNLF. Theoretically, the degenerated FWM process in single-mode HNLF can be properly described by the generalized nonlinear Schrödinger equation (NLSE)[8]

$$\frac{\partial U}{\partial z}+\frac{\beta^{(2)}}{T_0^2}\frac{\partial^2 U}{\partial \tau^2}=\mathrm{i}\gamma\left|U\right|^2 U, \tag{1}$$

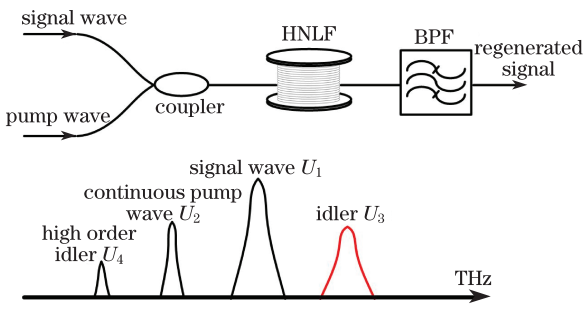

Fig. 1. Schematic of the all-optical amplitude reshaper.

where U is the complex electric field envelope of all the waves participating in the FWM, $\beta^{(2)}$ is the group velocity dispersion (GVD) given by the derivative of β, and the nonlinearity coefficient γ is given by

$$\gamma = \frac{2\pi n_2}{A_{\text{eff}}\lambda_{\text{ave}}}, \tag{2}$$

where A_{eff} and n_2 are the effective area and nonlinear refractive index of the adopted HNLF, respectively, and λ_{ave} is the average wavelength of the total wave envelope. To clearly describe the proposed scheme, the generalized NLSE is written in the form of coupled mode equations for the pump, signal, and idler waves under the quasi-continuous wave assumption

$$\frac{\mathrm{d}U_j}{\mathrm{d}z} = -\frac{\alpha}{2}U_j + \mathrm{i}\gamma\Big\{(|U_j|^2 + 2\sum_{k\neq j}|U_k|^2)U_j + \sum_{k,m,n} d_{k,m,n}U_kU_mU_n^*\mathrm{e}^{\Delta\beta_{kmn}}\Big\}, \tag{3}$$

where α is the attenuation coefficient of the fiber; j,k,m,n=1, 2, 3, 4, k, $m \neq n$; $\sum_{k,m,n}$ denotes all the possible permutations of the indices k,m, and n that satisfy $\omega_j - \omega_k = \omega_m - \omega_n$; $\Delta\beta_{kmn}$ indicates linear phase mismatching corresponding to indices k, m, and n. The degeneracy factor $d_{k,m,n}$=1 for $m = n$ and $d_{k,m,n}$=2 for $m \neq n$. Equation (3) shows that the evolution of the degenerated FWM process is affected by the SPM- and XPM-induced nonlinear phase shifts, as described by the second and third terms in the right-hand-side (RHS) of Eq. (3). Moreover, nonlinear phase shift terms are imaginary polynomials acting as functions of the pump power, signal, and generated idler waves. Thus, the contributions of SPM and XPM to the evolution of the FWM process should be as a quasi complex exponential function of the incident pump power.

In Fig. 2, the evolutions of conversion efficiency η=10 $\log_{10} P_3$.P_1 are plotted using the numerical solutions of Eq. (3) obtained by conducting the fourth order Rung-Kutta algorithm. Parameters used in the calculation are listed in Table 1. The signal power is 1 mW (0 dBm). Here, P_1 and P_3 denote the peak power of U_1 and U_3. During the calculation, coupled mode equations are truncated into four modes: two pump waves and two first order idler waves; higher order idlers are neglected due to their much lower intensity. Figure 2 clearly shows that η evolves as a quasi-complex exponential (or quasi-sinusoidal) function of P_1. Moreover, the evolution of η varies significantly for different FWM operational points

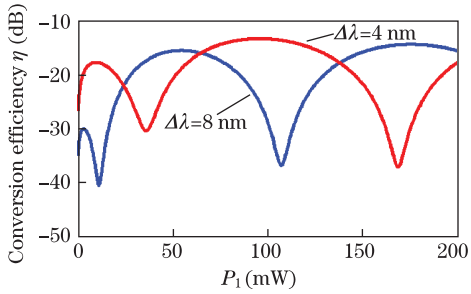

Fig. 2. Evolution of FWM conversion efficiency as a function of incident signal power.

Table 1. Parameters used in Theoretical Calculation

Parameter	Value
Signal Wavelength (nm)	1 544.5
Fiber Length (km)	3
Zero Dispersion Wavelength (nm)	1 554
Dispersion Slope (ps/(nm^2·km))	0.02
Nonlinear Coefficient (W^{-1}·km^{-1})	20
Loss Coefficient (dB/km)	0.26

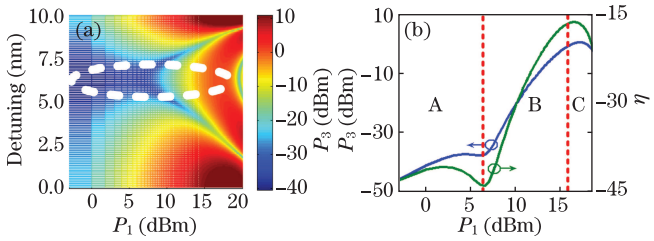

Fig. 3. (a) Generated idler power P_3 as a function of the incident pump power P_1 and the pump-signal detuning $\Delta\lambda$. (b) PTF and η with $\Delta\lambda$=6.75 nm.

(e.g., $\Delta\lambda$=4 and 8 nm). Most importantly, the evolutions of η under certain FWM operational conditions can bring about an enhanced performance for all-optical amplitude reshaping. In the following paragraphs, the enhanced reshaping performance is presented and analyzed.

In Fig. 3(a), the power of the idler power P_3 is plotted as a function of the signal power η and pump-signal wavelength detuning $\Delta\lambda$, again using the numerical solutions of Eq. (3). The parameters used in the calculation (listed in Table 1), such as the fiber length L, nonlinear coefficient γ, the zero-dispersion wavelength, and dispersion slope of the HNLF, are judiciously configured in order to obtain an optimized performance. Figure 3(a) shows that enhanced S-shaped PTFs can be obtained with $\Delta\lambda$ of 6.75 nm (highlighted with a white ellipse). In Fig. 3(b), detailed η and the corresponding PTFs between P_3 and P_1 with $\Delta\lambda$=6.75 nm are plotted, in which the principle of the optimization is evidently revealed. Particularly, at the beginning of the PTF (region A in Fig. 3(b)), η decreases as a function of incident signal power P_1, and the befitting destructive interaction between the two variables (η and P_1) brings about a flat curve in the PTF. The average slope to the parametric PTF is defined as

$$S_{\text{av}} = \log_{10}\Delta P_3/\log_{10}\Delta P_1. \tag{4}$$

The average slope in region A is measured as S_{av}(A)≈0.5<1; after η reaches its minimum at the end of region A, it rebounds to increase as a function of P_1, and the constructive interaction between η and P_1 causes a steep rise (S_{av}(B)≈4>1) within region B. After reaching its maximum at the end of region B, η decreases again, resulting in a flat plateau in region C (S_{av}(C)≈0.6<1). Thus, a full S-shaped PTF is obtained within a quasi period of η's evolution.

In summary, the proposed scheme has three strengths. First, two flat curves are obtained in PTF at lower and higher power levels in a single FWM stage, which can

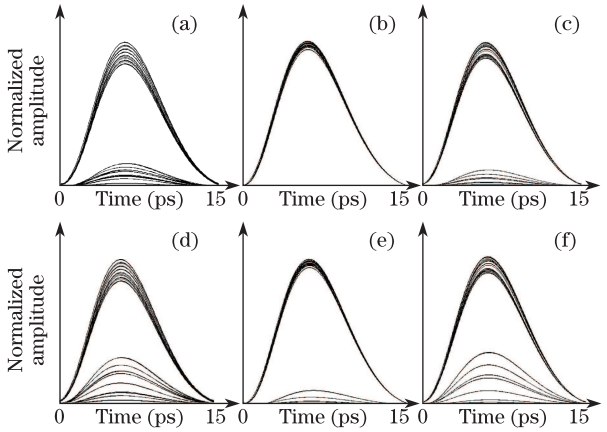

Fig. 4. Simulation results. (a) Normalized eye diagram of degraded input signal with ER=8 dB, and the corresponding reshaped signals (b) with and (c) without optimization. (d) Normalized eye diagram of degraded signal with ER=5 dB, and the corresponding reshaped signals (e) with and (f) without optimization. Parameters used in this simulation are listed in Table 1.

realize excellent ghost pulse and AJ suppression with a single FWM stage. Second, owing to constructive interaction between η and P_1, the average slope of the PTF in region B is large, thereby obtaining significant ER improvement. Third, the plateau in the PTF, which appears when P_1 reaches 15 dBm, is obtained through the counteraction of η and P_1 instead of pump depletion, removing the necessity of reaching the high pump depletion threshold for AJ suppression of marks. The input signal U_1 needs to be boosted by optical amplifiers, during which amplified spontaneous emission (ASE) noise may be introduced. However, with the ASE noise distributed through a wide spectrum and with random polarization, the FWM efficiency of the ASE noise can be much lower than that of U_1. Therefore, ASE noise is not considered a fatal problem for the practical utilization of the proposed scheme. Moreover, the enhanced S-shaped PTF for amplitude reshaping consists of a special set of solutions of the NLSE under certain operational conditions. Analogous to optic soliton propagation in fibers, any disturbance and saltation of the operational condition can influence the solutions. Therefore, the FWM operational conditions, especially the parameters of HNLF, are suggested to be maintained stable to achieve favorable reshaping performance.

The proposed optimization scheme is simulated by numerically solving the NLSE Eq. (1) using the split-step Fourier method; 40 Gb/s return-to-zero on-off keying (RZ-OOK) signal waves carrying a pseudorandom bit sequence of 15 ps chirp-free Gaussian pulses are used as the data pattern in the simulation. The peak power of the input data wave P_1 and continuous wave P_2 is 16 and 0 dBm, respectively. The data pulses are degraded by 20% of peak-to-peak amplitude jitters both on marks and spaces, and the extinction ratio is set at 8 dB. A normalized eye diagram of the input signal is shown in Fig. 4(a). Other parameters used in the simulation are identical with those listed in Table 1. Figure 4(b) shows the eye diagram of the reshaped signal using the proposed amplitude reshaping scheme. The ER and Q-factor of the reshaped signal improves to 14.4 and 7.8 dB, respectively. In order to emphasize the advantage of the proposed scheme, the reshaping performance of the proposed reshaper is compared with that of conventional FWM-based reshaper described in Ref. [6]. The ER and Q factors are measured to improve by only 2.3 and 1.8 dB, respectively, using the conventional reshaper, as shown in Fig. 4(c), much smaller than those obtained with the proposed scheme. Moreover, due to the large slope in region B of the PTF, ghost pulses on spaces can be obscured substantially even if the power of the spaces is located within region B. The benefit of this property is that the required ER of the input signal for amplitude reshaping is relaxed. Figures 4(d) and (e) show the initial and reshaped eye diagram of a 5-dB ER degraded signal. ER and Q-factor are improved by 9.1 and 5.8 dB, respectively, with the optimized reshaper, compared with their improvement of 0.7 and 0.4 dB, respectively, with the conventional reshaper, as shown in Fig. 4(f).

In conclusion, the performance optimization for all optical amplitude reshaping via fiber degenerated FWM is described. Optimization is achieved through the influence of SPM and XPM-induced nonlinear phase shifts on the evolution of FWM conversion efficiency. We numerically demonstrate the proposed reshaper with 40-Gb/s RZ-OOK signal and obtain much greater amplitude reshaping performance than conventional FWM-based reshapers.

This work was supported by the Fundamental Research Funds for the Central Universities and the National 973 Program of China (No. 2011CB301703).

References

1. P. V. Mamyshev, in *Proceedings of ECOC98* 475 (1998).
2. I. D. Philips, A. Gloag, P. N. Kean, N. J. Doran, I. Bennion, and A. D. Ellis, Opt. Lett. **22,** 1326 (1997).
3. R. Salem, M. A. Foster, A. C. Turner, D. F. Geraghty, M. Lipson, and A. L. Gaeta, Nat. Photon. **2,** 35 (2008).
4. E. Ciaramella and S. Trillo, IEEE Photon. Technol. Lett. **12,** 849 (2000).
5. E. Ciaramella, F. Curti, and S. Trillo, IEEE Photon. Technol. Lett. **13,** 142 (2001).
6. A. Bogris and D. Syvridis, J. Lightwave Technol. **21,** 1892 (2003).
7. T. Yamamoto and M. Nakazawa, IEEE Photon. Technol. Lett. **9,** 327 (1997).
8. D. Hart, A. Judy, R. Roy, and J. Beletic, Phys. Rev. E **57,** 4757 (1998).